Extended Crossover Model for Human-Control of Fractional Order Plants

MIGUEL MARTÍNEZ-GARCÍA [ID], TIMOTHY GORDON, AND LEI SHU, (Senior Member, IEEE)

School of Engineering, University of Lincoln, Lincoln LN6 7TS, U.K.

Corresponding author: Miguel Martínez-García (mmartinez@lincoln.ac.uk)

ABSTRACT A data-driven generalization of the crossover model is proposed, characterizing the human control of systems with both integer and fractional-order plant dynamics. The model is developed and validated using data obtained from human subjects operating in compensatory and pursuit tracking tasks. From the model, it is inferred that humans possess a limited but consistent capability to compensate for fractional-order plant dynamics. Further, a review of potential sources of fractionality within such man–machine systems suggests that visual perception, based on visual cues that contain memory, and muscular dynamics are likely sources of fractional-order dynamics within humans themselves. Accordingly, a possible mechanism for fractional-order compensation, operating between visual and muscular subsystems, is proposed. Deeper analysis of the data shows that human response is more highly correlated to fractional-order representations of visual cues, rather than directly to objective engineering variables, as is commonly proposed in human control models in the literature. These results are expected to underpin future design developments in human-in-the-loop cyber-physical systems, for example, in semi-autonomous highway driving.

INDEX TERMS Human-in-the-loop systems, data-driven modeling, cyber-physical systems oriented control, fractional order control, vehicle automation.

I. INTRODUCTION

A. BACKGROUND

This paper revisits a fundamental control problem for human-in-the-loop Cyber-Physical Systems (CPS) [1] – how humans control the motion of machines via visual perception and neuromuscular response in Fig. 1. Part of the motivation for this work is the growing interest in the control of autonomous and semi-autonomous ground vehicles, in particular the need to ensure human-machine system performs safely and effectively on the one hand, and for automated vehicles to behave in ways that are predictable and acceptable to other human drivers [2]. There is of course a rich classical literature on the general topic, but the modeling and understanding of human neuromuscular dynamics has developed over the years [3] [4], as have the signal processing and optimization techniques available to perform diagnostic analysis of experimental results [5] [6].

Traditionally in the literature on man-machine systems, humans are assumed to respond to objective machine output variables, which might be translational or angular displacements, ratios of such variables and their future predictions [7] [8], or visual field information derived from the *focus of expansion generated by the motion of a vehicle* [9]. Until now, little attention has been given to the question of how this variables are processed by the visual system and the central nervous system prior to the generation of a response action. Further, there has been little research into the manner in which *memories* of these inputs are used in human control. In this paper an in-depth analysis is made on both topics in the context of a simple laboratory control task.

B. RELATED WORK

With the broader objective in mind, research conducted over 50 years ago is revisited in this paper, and in particular McRuer's Crossover (CO) model [10], perhaps the most common example of a human control model, is taken as a benchmark. The CO model (see Section II-B) describes how humans adapt to different plants to elicit stable and effective control responses. In this classical CO model, the input is represented directly as a displacement error between a target and a human-controlled follower. Similarly in [11], where another class of models is formulated using optimal control theory, the input to the human controller is represented as an objective 'engineering' variable. While optimal control methods

are often effective at performing machine control, the link to human performance is not clear. The same difficulty is found in a more recent scheme for reproducing human-control performance: deep reinforcement learning [12]. By contrast, while the CO model only offers a good description of the human over a certain range of frequencies, it is simple and interpretable.

In the area of driver modeling (i.e. human control of highway vehicles, most specifically steering control) many techniques from control theory and human performance modeling have been applied – for reviews of such models see [13], [14]. Driver models can be broadly divided into those based on optimal control, e.g. [15], and those based on the feedback of error from previewed target points, e.g. [16]. Again, optimal control methods can achieve high quality tracking performance, but are not strongly connected to human performance. Examples include Macadam's model [15] where the human is assumed to act as a linear optimal controller after a certain response delay, and that of Prokop [17] where the steering control task is formulated as a path optimization problem.

Preview models can be divided into single and multiple point preview models according to their number of inputs [18]. For example, Kondo's model uses a prediction of the lateral offset after a given preview time [16].

Salvucci and Gray [19], on the other hand, proposed a model based on a two-point control strategy. Similar to this, the CO model was itself adapted to construct a virtual-driver [20].

Further approaches have made use of neural networks [21] or deep learning [22] to achieve human-level performance control. But, as with optimal control methods, such 'black box' approaches do not provide much insight or information about the characteristics of human control. And in all the cited cases the model adopts objective 'engineering variables' as input and does not explicitly consider memory aspects, although some memory storage may be still present in these models as a byproduct of the modeling strategy.

C. CONTRIBUTION

The motivation for incorporating explicit memory modeling and identification of memory-based variables in human-control comes from established neuroscience research; for example, humans are known to keep a saccadic record between tracking eye movements while observing their environment [23]. Models in neuroscience suggest that neurons can be modeled as integrators of past elements of information [24]. And the muscular system displays a memory component in its behavior too [4].

It is widely known that the response of a system modeled by ordinary differential equations (equivalently, in the linear case, modeled by transfer functions) to any given input is determined by a single vector of initial condition states. For instance, in a mechanical system, these are usually the generalized position and velocity variables that describe the available degrees of freedom. On the contrary, it seems natural than human tracking behavior, and biological systems in

general, elicit a response based on a series of past observations. In [25], the limitations of classical linear models for the particular case of steering control are shown.

Thus a mathematical approach that explicitly includes memory processes is motivated. With this purpose in mind, the method of fractional calculus is considered, based on the property that fractional derivatives add memory processes to a dynamical system [26]; one example of modeling memory with fractional calculus is its application to electronic components [27] [28]. And to test out the relevance of fractional-order dynamics to human control performance, experiments are conducted on human tracking behavior for plants which have the dynamic characteristics of fractional-order systems. Further motivation for considering this approach is that fractional operators introduce wider power law behavior into the frequency spectrum of a system; for example it is known that pink noise occurs naturally in biological systems [29].

Hence, in the following work, a generalization of the CO model has been introduced by analyzing human response to plants of fractional-order, which we refer to as the *Fractional Crossover Model* (FCO model). The intention is as follows: (*i*) to test if humans can interact in a coherent way with fractional-order plants; (*ii*) to formulate a generalization of the CO model that accounts for memory behavior in the system; (*iii*) to investigate potential sources of fractionality or memory behavior in real man-machine systems; (*iv*) to test whether humans can compensate for the fractionality of a system and hence simplify the overall human-machine dynamics; (*v*) to investigate whether fractional-order dynamics are inherent within the human control; (*vi*) to introduce the theory of fractional calculus to human-machine systems and driver behavior modelers.

The paper is structured as follows: in Section II the required mathematical background for this research is summarized (the theory of fractional calculus and the CO model), while in Section III the details of human performance experiments and data collection are discussed. Then, in Sections IV and V we perform in-depth data analysis to elicit the contributions of memory and perception effects on control performance, and finally, in Section VI the conclusions are outlined and the potential implications of this research are discussed.

II. BACKGROUND
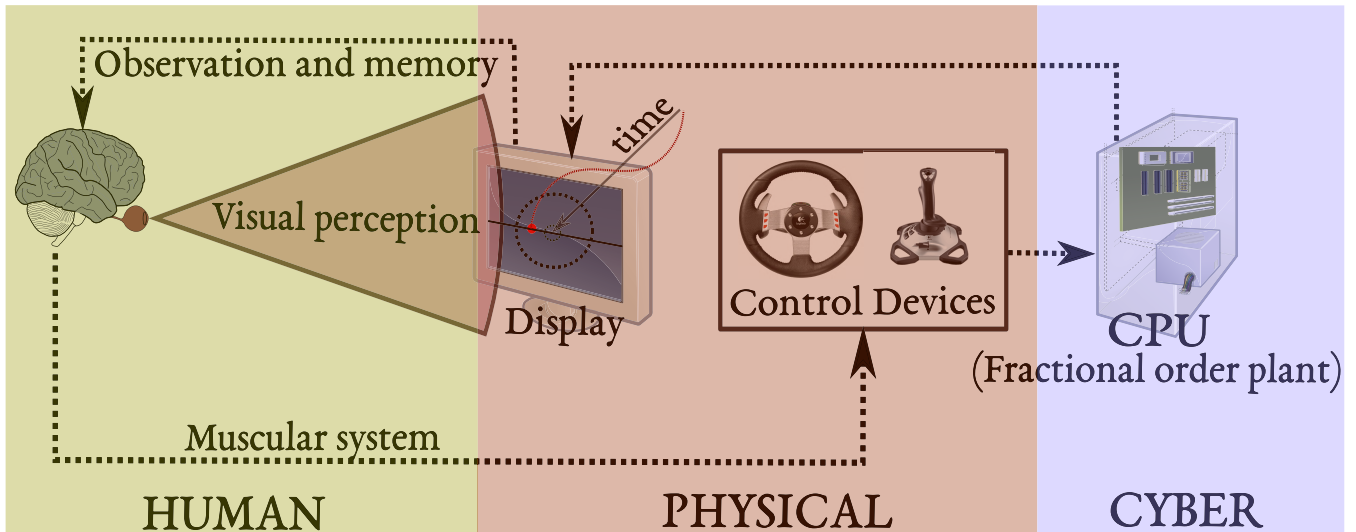### A. OVERVIEW OF FRACTIONAL CALCULUS FROM A 'MEMORY' PERSPECTIVE
1) THE FRACTIONAL DIFFERENTIAL AND INTEGRAL OPERATOR

The Laplace transform of successive derivatives of a function $D^n f(t) = f^{(n)}(t)$, when the initial conditions are zero, is known to be

$$\mathcal{L}\{D^n f(t)\} = s^n F(s). \tag{1}$$

For nested integrals $D^{-n} f(t) = \int_0^t dt_1 \int_0^{t_1} \cdots \int_0^{t_{n-1}} f(\eta)\, d\eta$,

$$\mathcal{L}\{D^{-n} f(t)\} = F(s)/s^n. \tag{2}$$

From equations (1) and (2) it can be inferred that transfer functions, corresponding to derivative or integral operators, always yield a magnitude frequency response with a slope multiple of 20 dB/decade. The phase response is always a multiple of $\pi/2$ rad. Nevertheless, 'colored' noise with frequency spectrum $1/f^\alpha$ $\alpha \in (0, 2)$ seems to occur generally in complex systems, particularly in human response. Measurements of mental noise and human tracking behavior have shown magnitude frequency responses with slopes that are not multiples of 20 dB/decade [26] [30].

To represent this behavior, transfer functions with additional terms can be used, although this results in having multiple additional free parameters to be fitted. Then there is the alternative of considering simple transfer functions with fractional exponents: s^α for $\alpha \in \mathbb{R}$. From (1) and (2) it can be extrapolated that this is equivalent to employing non-integer powers of the differential operator:

$$\mathcal{L}\{_0D_t^{-\alpha}f(t)\} = F(s)/s^\alpha, \quad \alpha \in \mathbb{R}. \tag{3}$$

In fact, as it is known that[1] $\mathcal{L}\{t^{\alpha-1}/\Gamma(\alpha)\} = 1/s^\alpha$ and by using the Convolution Theorem it is inferred that

$$_0D_t^{-\alpha}f(t) = \mathcal{L}^{-1}\{\frac{1}{s^\alpha}F(s)\} = \frac{1}{\Gamma(\alpha)}\int_0^t f(t)(t-x)^{\alpha-1}\,dx. \tag{4}$$

Equation (5) coincides with the definition of the Riemann-Liouville fractional integral [26].

Definition 1 (Riemann-Liouville Fractional Integral): If $\alpha \in \mathbb{R}^+$ and f is a piecewise continuous function on the interval $(0, T]$, with $T \in \mathbb{R}^+$, and f is integrable on the interval $[0, T]$, then for $t \in (0, T]$

$$_0D_t^{-\alpha}f(t) = \frac{1}{\Gamma(\alpha)}\int_0^t f(t)(t-x)^{\alpha-1}\,dx \tag{5}$$

is the Riemann-Liouville fractional integral of order α at t.

To perform fractional differentiation of order $\nu > 0$ it is only needed to compose conventional differentiation with fractional integration:

$$_0D_t^\nu f(t) = D^{\lceil\nu\rceil}\{_0D_t^{\nu-\lceil\nu\rceil}f(t)\}, \tag{6}$$

where $\lceil x \rceil$ represents the ceiling function.

There are different definitions of the fractional differential operator [31] [32]. The most common are the Riemann-Liouville and the Grünwald-Letnikov definitions, which are equivalent to each other for smooth functions. The Riemann-Liouville fractional operator displays clearly the non-locality of the operator – even fractional differentiation is defined through an integral – and its frequency spectrum characteristics. The Grünwald-Letnikov fractional operator shows that fractional differintegration can be expressed as the sum of a time series. It follows from the expression to define classical derivatives from backward differences,

$$D^n f(t) = \lim_{h\to 0}\frac{1}{h^n}\sum_{m=0}^n (-1)^m \binom{n}{m} f(t-mh), n \in \mathbb{N} \tag{7}$$

that can be extended to non-integer order of differentiation and integration [33] by using the gamma function.

---

[1]Where $\Gamma(z) = \int_0^\infty x^{z-1}e^{-x}\,dx$ is the gamma function which generalizes the factorial operation to non-integer values – it satisfies $\Gamma(z) = (z-1)\Gamma(z-1)$ $\forall z \in \mathbb{C} \setminus \{\mathbb{Z}^- \cup \{0\}\}$.

Definition 2 (Grünwald-Letnikov Fractional Operator): [2]

$$_0D_t^\alpha f(t) = \lim_{h \to 0} \frac{1}{h^\alpha} \sum_{m=0}^{t/h} \frac{\Gamma(m-\alpha)}{\Gamma(-\alpha)m!} f(t-mh), \ \alpha \in \mathbb{R}\backslash\mathbb{N}. \quad (8)$$

Equation (8) can be approximated with its discretized counterpart:

$$_0\widetilde{D}_t^\alpha f(t) = \frac{1}{h^\alpha} \sum_{m=0}^{t/h} \frac{\Gamma(m-\alpha)}{\Gamma(-\alpha)m!} f(t-mh), \ \alpha \in \mathbb{R}\backslash\mathbb{N}. \quad (9)$$

The last expression, essentially a linear filter, displays clearly that the fractional operator is a weighted sum of past observations and therefore it is an operator with memory. This is unlike the classical derivative which provides only local information. Thus the limits of integration (here 0 and t), must be specified also when applying fractional derivatives – left and right subscripts in (8). Equations (3) and (8) underlie the relationship between power spectrum slope and memory.

There are other ways in which a dynamical system holds memory. The states of a system are memory variables themselves, as well as transport delays. Memory can also be held in a dynamical system in a cumulative manner, such as a mean of previous states, an integrator, a Bayesian model [34] or a Kalman filter. This last approach has been considered in human control to design optimal control models [11]. However, the fractional operator models memory in a more natural form: it considers a memory history of every past state which decays through time. The weights in (8) satisfy the property that recent states of the system are more relevant than older events. Besides, as fractional calculus is included within the framework of differential equations, it is a very practical way to include memory while modeling dynamics. In addition, a fractional operator characterizes its memory properties with only one parameter.

2) APPROXIMATION ERROR OF FRACTIONAL DERIVATIVES
It can be proved [33] that the discretization error when computing $_0\widetilde{D}_t^\alpha f(t)$ satisfies[3]

$$_0D_t^\alpha f(t) - _0\widetilde{D}_t^\alpha f(t) = \mathcal{O}(h). \quad (10)$$

The truncation error, by considering only a finite memory window of width L can be bounded as follows:

$$|_0D_t^\alpha f(t) - _{t-L}D_t^\alpha f(t)| \leq \frac{ML^{-\alpha}}{|\Gamma(1-\alpha)|} \quad (11)$$

where M is a bound for $|f|$. Equation (11) is referred to as the *short-memory principle* and encapsulates the idea that recent events are more relevant that distant ones. Thus by choosing L such that $ML^{-\alpha}/|\Gamma(1-\alpha)| \approx h$ the total approximation error is $\mathcal{O}(h)$.

---

[2]Generalized from (7) by using the property:
$\Gamma(n-z)\Gamma(z-n+1) = (-1)^n\Gamma(-z)\Gamma(1+z)$ for $z \in \mathbb{C}$ and $n \in \mathbb{N}$. The expression in the definition cannot be evaluated when α is a positive integer, which corresponds to classical differentiation, because the gamma function has a pole in every negative integer.
[3]For analytic functions.

3) FRACTIONAL DIFFERENTIAL EQUATIONS
From (3) an equivalence between fractional differential equations and transfer functions can be established. In particular the following case is considered:

$$\frac{Y(s)}{U(s)} = \frac{K}{s^\alpha(Ts+1)}$$
$$\Updownarrow$$
$$T_0D_t^{\alpha+1}y(t) + _0D_t^\alpha y(t) = Ku(t). \quad (12)$$

Substituting (9) into (12) and reorganizing terms yields:

$$f(t) = \frac{1}{T+h}\Big[h^{\alpha+1}Ku(t) - T\sum_{m=1}^{t/h}\frac{\Gamma(m-\alpha-1)}{\Gamma(-\alpha-1)m!}f(t-mh)$$
$$- h\sum_{m=1}^{t/h}\frac{\Gamma(m-\alpha)}{\Gamma(-\alpha)m!}f(t-mh)\Big] + \mathcal{O}(h). \quad (13)$$

By using (13) in a step-wise manner, equation (12) can be numerically integrated with a local discretization error $\mathcal{O}(h)$. While there exist higher order algorithms to approximate fractional derivatives and for numerical integration of fractional differential equations [32] [35], for use in human-in-the-loop interactions and real time application the method in Equation (13) seems to be the most appropriate. Also, there is little risk of drift arising from any approximation error, since the human operator is constantly canceling errors when performing closed-loop control.

In the recent literature, the topic of fractional order control has gained increasing attention, due to its capability to model higher order behavior. For example, in [36] a fractional order observer is considered to control fractional order plants, and in [37] fractional PID controllers are employed to design rail vehicle tilt controllers.

B. CROSSOVER MODEL
The CO model describes the combined action of a human operator and a controlled plant within a restricted range of frequencies. The model was deduced by recording responses of human subjects to visually presented stimuli in single-loop tracking tasks [38]–[40]. In the original experiments, human subjects were requested to control a moving element in a display by means of a control stick held between thumb and forefinger. The position of the moving element represented an error, which was induced by a quasi-random forcing function. Test subjects were requested to minimize the error by moving the controlled element towards a reference point in the center of the display. The control actions that the human performs over the moving element – with known dynamics given by a chosen transfer function – places the human as a serial element inside the control loop (Fig. 2a).

It was observed that the manipulative control actions of the human operator are different for different transfer functions, but the combined human-machine behavior is approximately invariant. Thus the CO model exhibits a behavioral invariant of the human in its effort to adapt to the plant, offering a consistent human-machine behavior. What characterizes the

(a)

(b)
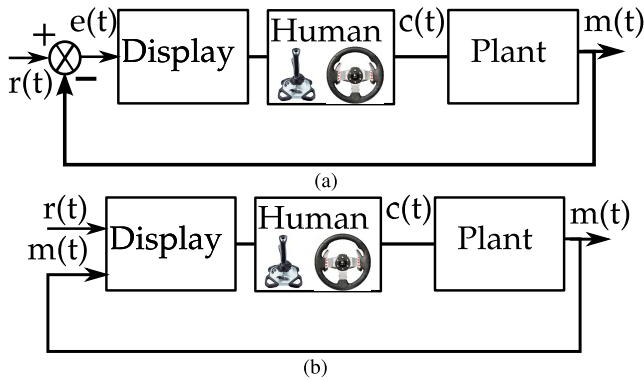
FIGURE 2. Human-machine control loop as in the classical and the here presented experiments for each display mode: (a) compensatory and (b) pursuit.

human controller is its dexterity in different contexts. The model is expressed as a product of transfer functions for the combined human-machine system and is characterized by just two parameters: the *crossover frequency* ω_c and a time constant τ, which represent the combined control gain and the effective time delay respectively. The effective time delay characterizes the sum of the neuromuscular lag and the transport delays of the system. The open-loop transfer function for the forward path in the CO model is

$$Y_h(s) Y_p(s) = \frac{\omega_c e^{-\tau s}}{s}, \qquad (14)$$

where Y_h represents the human operator and Y_p the plant. As mentioned, ω_c is both the crossover frequency and the system gain. The amplitude and phase response for the model are:

$$\mathbf{A}(\omega_f) = 20(\log \omega_c - \log \omega_f) \quad \text{dB.} \qquad (15)$$

$$\Phi(\omega_f) = -\pi/2 - \tau \omega_f \quad \text{rad.} \qquad (16)$$

One important aspect of the model is that it accurately represents human behavior only in the vicinity of ω_c. But this is sufficient to ensure closed-loop stability and transient performance, via the gain and phase margins, i.e. via the open-loop responses in the vicinity of the crossover frequency. The CO model is a linear approximation of a system that is nonlinear and complex, at least in the human part. The error of approximation between the linear model and the recorded human output is called the *remnant*. This combination of linear part plus noisy remnant constitute the theory of *quasi-linear* models [7]. The CO Model, since it was introduced, has been continuously used in human performance and control research, one example being its application to vehicle steering control [10] [41].

C. MECHANISMS IN VISUAL MEMORY
This section considers the question of which information the human-operator collects and responds to from the perceived visual input. Motion detection is one of the oldest acquired visual capacities; it is essential to make predictions while tracking a moving target. It would be unfeasible to detect motion without some type of pre-filtering that compares stimuli perceived at different instants. As a mechanism of motion detection, it has been proposed to result from temporal delay filtering [42]. Thus motion detection involves integration of past visually perceived inputs; it is a process with memory. Besides motion detection, the following reported mechanisms illustrate that memory processes are inherent in the visual system:

1) TRANS-SACCADIC MEMORY
In the human eye, the *fovea centralis* provides the maximum resolution of receptors within the retina, but this only spans a field of view of 2-3 degrees. Consequently, the eye usually moves actively and selectively to sample the surroundings. Humans redirect their gaze about three times per second. This allows for the different objects in the visual field to be projected into the foveal region [43]. However, even if vision consists of a chain of discrete actions, we perceive the environment as a unified continuous image. It has been verified that a *trans-saccadic memory* is retained during saccadic periods. During each saccadic period visual perception is temporarily halted and humans are basically blind [44]. But changes in natural scenes during saccadic periods are detected after the saccade [23]. As a result, even the initial stages of visual perception involve some kind of memory.

2) LINEAR-NONLINEAR MODELS
Encoding models in neuroscience use linear filters to represent trains of neuron spikes produced by time-varying input stimuli. In these models, the output firing rate is approximated by a linear filter in time followed by a non-linear transformation in cascade [24]. Although these models in general don't offer a direct relationship between biological parameters and fitted parameters, the success in the approach implies that neurons can be modeled as integrators of temporal information. Thus it can be inferred that visual response is based on an aggregate of stimuli perceived at different instants.

3) OCULOMOTOR NEURONS
In [3] it is proposed that the dynamics of motor and premotor neurons in different oculomotor subsystems, which lead to pursuit saccades, are of fractional nature. One particular case is the vestibulo-oculomotor system, which counteracts head rotation with eye rotation to maintain a steady image in the visual field [45]. The fractional attributes of these neurons suggest that there is a memory component in visual tracking.

In view of the above, it seems reasonable to propose a model which introduces memory effects via fractional-order dynamics within the human control model – whereby the human operator integrates past observations to produce a response from a combination of visually perceived inputs over a finite time-window. And to test and validate the proposal, it is also appropriate to expand the dynamics of the

plant being controlled to include the option for fractional-order dynamics.

III. EXPERIMENTAL SETUP AND METHODS
A. COMPENSATORY AND PURSUIT MODES
Within the existing literature on human control, two similar control tasks are commonly tested: compensatory mode and pursuit mode [46] [47]. Both display modes are considered in the following data collection experiments. The main difference between the modes is in the number of moving elements presented in the display. In compensatory mode, there is only one moving element in addition to one fixed reference point. The error $e(t)$ is represented as the Euclidean distance between the moving and the fixed elements. The task of the human operator is to minimize $e(t)$ by means of a control device, which allows them to generate an input to the plant – with transfer function Y_p. The error is the difference between a quasi-random forcing function $r(t)$ and the plant output $m(t)$ (Fig. 2a). Hence, in compensatory mode only the relative error is seen by the human, who does not have direct access to the plant output. The position of the moving object results as the joint effect of the forcing function, the human response and Y_p acting in closed-loop.

In pursuit mode there are two moving elements. The reference point now moves according to the forcing function $r(t)$, and does not depend on the human manipulative control actions. The other moving element, controlled by the human, displays the plant output $m(t)$. In this case neither one of the moving elements directly represents $e(t)$, but the error is again perceived as the Euclidean distance between the two moving elements (Fig. 2b).

B. HUMAN-IN-THE-LOOP TRACKING EXPERIMENTS
A number of human tracking experiments were recorded from ten subjects of mixed gender, whose ages spanned from 22 to 33 years. In each of the experiments, four signals were recorded: the forcing function $r(t)$, the plant output $m(t)$, the error signal $e(t)$ and the human response $c(t)$ (Fig. 2). The controlled moving element was presented on a computer monitor as a circular solid dot, which varied in color for each plant considered, so that the subjects were aware of a change in the dynamics and thus the adaptation time was shortened. The reference point was displayed as a circle of slightly larger size and different color. Besides the two display modes, the tracking experiments were performed according to other variants: two different control devices (a joystick and a steering wheel) and five different plants.

Each participant performed 4 experiments consisting of a round of 5 tracking 'events' of 90 s duration Table 1, each event with a different plant. The considered transfer functions for each plant are given in Equation (12) with $\alpha = 0.5, 0.75, 1, 1.25, 1.5$ (and $T = 0.1$). The order of the different plants was randomized for each subject. For each participant, half of the experiments were executed with a joystick and half with a steering wheel. Half of the subjects

performed the joystick experiments in compensatory mode and the steering wheel experiments in pursuit mode, while this was reversed for the other half. After each round the subjects were requested to rest. A training round of tests, which were not recorded, was performed prior to the actual tests in order to habituate the participants to the experimental setup.

The forcing function $r(t)$ was composed of a sum of sinusoids with a range of frequencies $f_k = 0.01 - 20$ Hz:

$$r(t) = \sum_{f_k \in \{0.01, 0.02, ..., 20\}} e^{-4f_k} \sin(f_k \cdot 2\pi t - \varphi_k) \quad (17)$$

where $\varphi_k \in [-\pi, \pi]$ is a randomized phase for each summation term. With this choice, the amplitude is negligible for frequencies outside of the range where a human-operator can perform adequate control. The choice of quasi-random forcing functions was based on the knowledge that humans find it difficult to perform adequate tracking when the forcing frequencies are greater than approximately 1 Hz [48].

The experimental data was sampled at 100 Hz. For each of the 90 s events, the initial 20 s were excluded, in case the subjects were adapting to the new plant dynamics. Another reason to exclude these initial data is to allow the fractional operators to populate their internal memory. Similarly the final 10 s were excluded, as during that time the forcing function was gradually returned to zero, to minimize discontinuity during a change in plant dynamics. Thus from each event, only 60 s of data are analyzed.

In nine of the recorded events it was observed that the magnitude of the frequency response (in dB) remains negative; hence no crossover frequency could be determined. Since these events do not reflect the normal characteristics of the human operator described by the CO model, they were regarded as non-representative and hence discarded from further analysis. The anomaly of these events may have been caused by different levels of attention or fatigue during the tests, though no systematic pattern of occurrence was noticeable.

IV. FRACTIONAL CROSSOVER MODEL (FCO MODEL)
A. MODEL DESCRIPTION
Firstly, the question of whether the human operator is able to interact and control fractional-order plants is examined. By fitting the CO model with the recorded data (Section III-B) corresponding to non-fractional ($\alpha = 1$) and fractional-order plants ($\alpha \neq 1$), it is shown that the invariance property of the CO model does not hold in the fractional case; the recorded event data corresponding to fractional order plants do not display the characteristic slope of -20 dB/decade of the CO model. An initial examination (Fig. 3) of a representative set of event data exhibits that the slope and phase conditions (15), (16) are no longer satisfied. By analyzing the particular cases the following pattern is observed [26]:

- For $\alpha = 1$ the classical CO model is consistently verified as described in [38] (Fig. 3b).

TABLE 1. Summarized experimental and data analysis parameters. (⋆) The frequencies of the forcing function are spaced every 0.01 Hz. Note that the frequencies are weighted so that they are only effective up to 0.5 Hz (17). The remaining frequency values are added to simulate noise in the system.

Experimental Parameters	
Number of subjects	10
Age of subjects	22-33 years
Duration of each event	90 s (60 analyzed)
Number of recorded events	200
Forcing function freq. range	0.01-20 Hz⋆
Sampling frequency	100 Hz
Steering wheel range	-450 to 450 degrees
Analysis Parameters (system identification)	
FFT window size	1024 samples≈10 s
FFT window overlap	512 samples≈5 s
Genetic algorithm # generations	2000
Genetic algorithm # population	500

TABLE 2. Average of the mean square error (MSE) for the recorded events between the frequency response in the data and each fitted model.

α	Crossover Model		FCO Model	
	MSE amp.	MSE ph.	MSE amp.	MSE ph.
0.5	0.063	0.162	0.021	0.033
0.75	0.025	0.034	0.018	0.019
1	0.119	0.099	0.090	0.067
1.25	0.010	0.163	0.009	0.045
1.5	0.018	0.252	0.009	0.106
Mean	0.047	0.142	0.029	0.054

- For $\alpha < 1$ the slope of the frequency response magnitude is greater than the -20 *dB*/decade predicted by the CO model. Besides, there is an additional positive constant shift in phase (Fig. 3a).
- For $\alpha > 1$ the slope of the frequency response magnitude is less than the predicted $-20dB$/decade. In this case there is an additional negative constant shift in phase (Fig. 3c).

In light of the above, a generalization of the CO model is proposed – the FCO model:

$$Y_h^\lambda(s)\,Y_p^\alpha(s) = \frac{(\omega_c)^\lambda e^{-\tau s}}{s^\lambda}. \qquad (18)$$

The model includes an additional parameter λ that reproduces the pattern described. $Y_h^\lambda(s)$ is the human transfer function and $Y_p^\alpha(s) = K/s^\alpha(Ts+1)$ is the plant. The amplitude and phase response for the FCO model are:

$$\mathbf{A}_\lambda(\omega_f) = 20\lambda(\log\omega_c - \log\omega_f)\quad \text{dB}. \qquad (19)$$

$$\Phi_\lambda(\omega_f) = -\pi/2\lambda - \tau\omega_f \quad \text{rad}. \qquad (20)$$

B. MODEL VALIDATION AND DEPENDENCE OF PARAMETERS

Comparing the results between the two models for different values of α, it is observed that the FCO model significantly
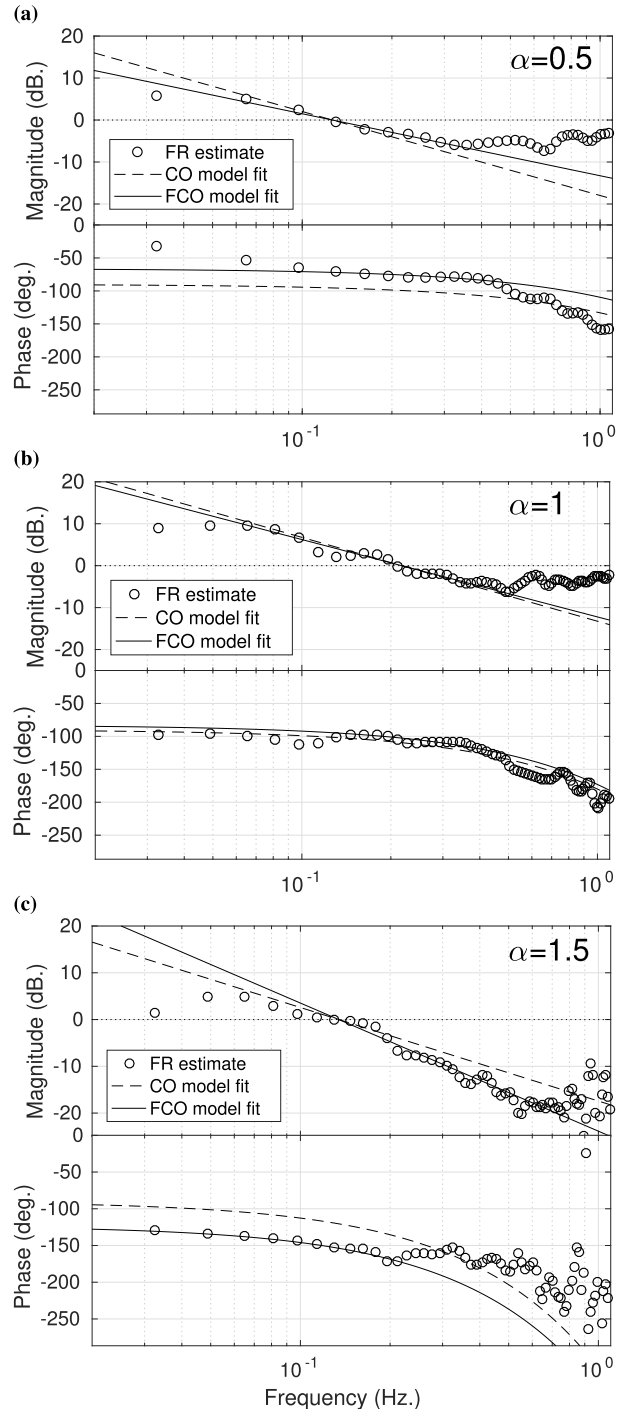
FIGURE 3. Frequency responses fitted to the classical CO model and the FCO model for three sample events (using the steering wheel and in pursuit mode). Plant transfer functions: (a) $\alpha = 0.5$, (b) $\alpha = 1$ and (c) $\alpha = 1.5$.

improves the fit (Table 2). The FCO model reduces the MSE by 38% for magnitude and 62% for phase.

The new parameter λ exhibits an approximate linear relationship with respect to α. In Fig. 4 the distributions of λ are fitted independently for each event and grouped according to α. The relationship is estimated by fitting a linear trend
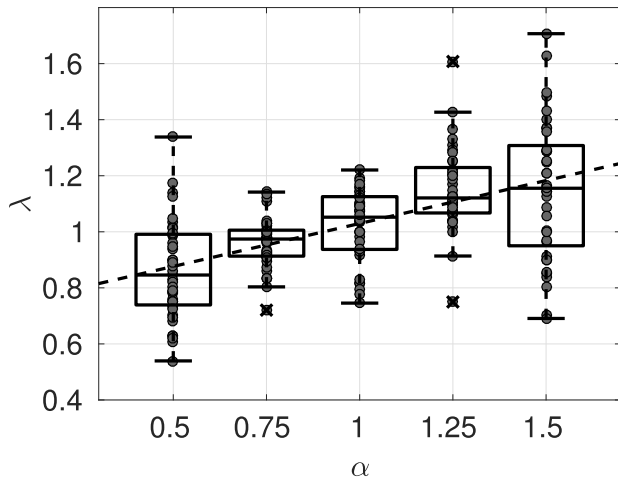
FIGURE 4. Distribution of the parameter λ, for all the events, and for each plant with their corresponding box plots. The limits of the boxes denote the 25% (q_1) and 75% (q_3) percentiles. The whiskers have a maximum length of 1.5 the interquartile difference ($q_3 - q_1$). Outside of this range the values are regarded as outliers. The median values are fitted with a dashed line.

FIGURE 5. Comparison of the effective time delay for the two tested control devices: joystick and steering wheel. The human operator is able to produce a quicker response with the joystick. The median values are 0.275 s and 0.34 s for the joystick and the steering wheel respectively.

to the median values for each fractional plant:

$$\lambda = m\alpha + c \approx m\gamma + 1 \tag{21}$$

and values $m = 0.31$, $c = 0.72$ are obtained. It is convenient to define $\gamma := \alpha - 1$ as a measure of how far the plant is from a non-fractional model – we may call this the *fractionality* of the plant. Accordingly, for these particular values of m and c, the FCO model can be rewritten as:
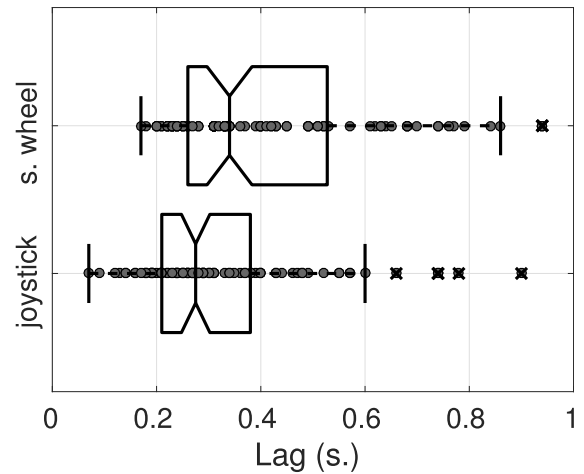
$$Y_h^\gamma (s) \frac{K}{s^{1+\gamma}(Ts + 1)} = \frac{(\omega_c)^{m\gamma+1} e^{-\tau s}}{s^{m\gamma+1}} \tag{22}$$

and hence, the response of the human operator is given by

$$Y_h^\gamma (s) = K^{-1}(\omega_c)^{m\gamma+1} s^{\gamma(1-m)}(Ts + 1)e^{-\tau s}. \tag{23}$$

The result $m \approx 0.3$ can be interpreted as follows: on average the human operator is able to compensate for about 70% the fractionality of the combined human-machine system. The compensation is represented in the model of the human (23) by an additional factor $\omega_c^{m\gamma} s^{\gamma(1-m)}$, not present in the CO model. Hence, the FCO model offers a suitable generalization of the classical CO model, describing human control of a wider category of plants. These may include complex and nonlinear plants or plants with hysteresis effects, and where a fractional order approximation can be determined (see for example Section V-A below). With the given data it is only possible to speculate about what may happen by further increasing the fractionality towards $\alpha = 2$. It seems natural that only the difference from α to the nearest integer order is relevant.

The frequency range of validity of the CO model is not reported in the classical literature [38], as it is dependent of the forcing function, the human response characteristics, the control device and the controlled plant. For the presented setup, it is observed that the CO and the FCO models are generally valid on the frequency range of 0.05-0.5 Hz.

C. STEERING WHEEL CONTROL

Concerning the applicability of the presented work to steering wheel control, longer neuromuscular lags are obtained with the steering wheel than with the joystick (Fig. 5); steering wheel control involves a higher participation of the musculoskeletal system. Nevertheless, the median MSE for the recorded events are very similar: 0.091 and 0.138 for the joystick and the steering wheel respectively. On the other hand, regarding the control of ground vehicles, the steering ratio in the steering system of a conventional vehicle (typically around 16:1) implies that steering wheel control provides superior directional precision compared to a joystick. For example, in [49] it is reported that the tracking performance is superior with a steering wheel than with a joystick for normal driving, but equivalent in crash avoidance maneuvers. While joystick control can yield a faster response, it is too sensitive to allow an intermittently-active driving attendance; it demands constant and quick readjustments.

D. DISCUSSION

It is known that the crossover frequency is larger for more skilled operators [26] [40]. Higher values of ω_c mean that stable tracking occurs across a higher frequency range. For example, lower control gains have been reported for inebriated drivers [50]. Examining the fitted values of ω_c for every α (Fig. 6), smaller values are observed in fractional-order plants. In particular ω_c seems smaller for larger $|\gamma|$, especially for higher order plants. Additionally, for $\alpha > 1$, the variability between the different events is seen to be smaller. This suggests that fractional-order plants are more difficult to control, and while for some events subjects were able to achieve relatively larger values of ω_c when $\alpha < 1$, for $\alpha > 1$ the crossover frequency is consistently smaller; the degree of difficulty in a tracking task also increases with the order of the plant.
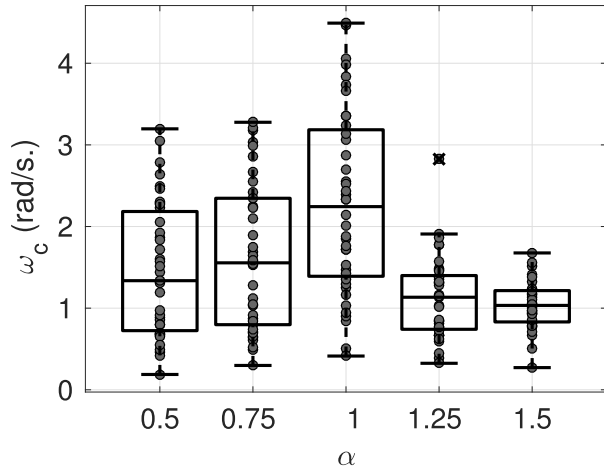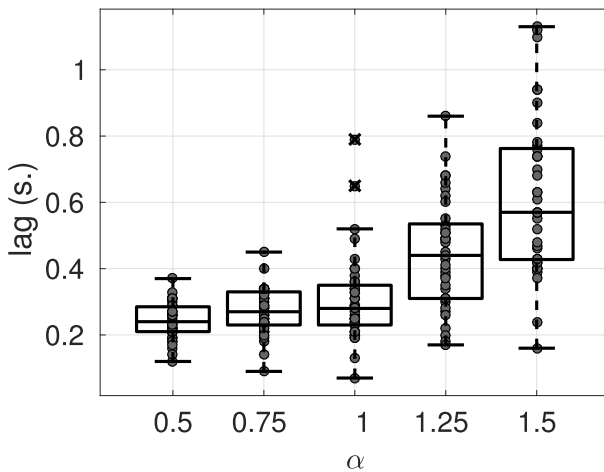
FIGURE 6. Distribution of the fitted ω_c values for all the studied events and for each plant. Smaller values of ω_c are generally observed for fractional plants ($\alpha \neq 1$), specially for the higher order ones.
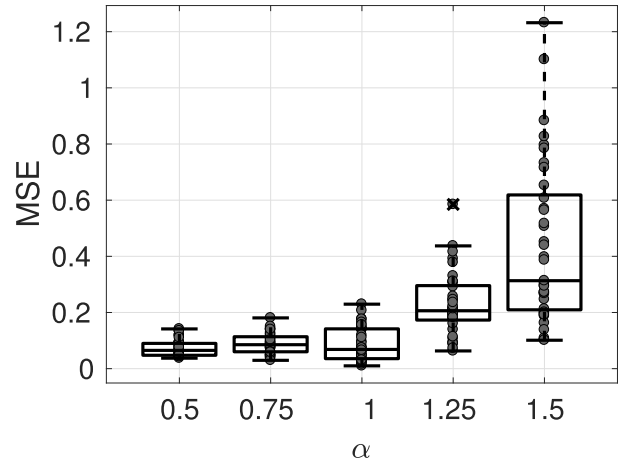
FIGURE 8. MSE of $e(t)$ for the events tabulated according to α. The performance is lower for the higher order plants and equivalent for lower order plants.

FIGURE 7. Distribution of the fitted effective time delay values τ for all the studied events and for each plant type. τ increases along with the order of the plant, especially for $\alpha > 1$.

Interestingly, while for $\alpha < 1$ the crossover frequency is smaller than for the non-fractional plant ($\alpha = 1$), the neuromuscular lag is very similar (Fig. 7). This indicates that, even when the subjects operate at lower bandwidth when controlling fractional-order plants, for $\alpha < 1$ the values of τ are similar to those in the non-fractional case. It may be that subjects are able to use the memory in the system to predict its behavior in the lower fractional order cases.

This is further supported by the fact that almost identical performance is found for $\alpha < 1$ and for $\alpha = 1$ – Fig. 8. On the other hand, the higher order plants ($\alpha > 1$) result in a higher error $e(t) = r(t) - m(t)$. For $\alpha = 1.5$ the variability in the data is significantly higher, which suggests that not all the subjects were able to fully adapt to the plant during the course of the tests.

The simplicity of the CO model relies on the fact that it depends on just two parameters (ω_c and τ), which have

an intuitive interpretation. The FCO model adds just one additional parameter: the fractional exponent of the combined human-machine system (λ). λ is therefore related to the memory in the whole system. Besides, λ also has an intuitive meaning: it determines the slope of the frequency spectrum and the added phase offset. Because λ depends on the plant, which in most cases will be known, the FCO model can still be considered a two parameter model.

Since fractional derivatives lie between two integer order derivatives, the results for $\alpha < 1$ suggest that humans can effectively combine information with different levels of differentiation. This is equivalent to combining input variables such as position and velocity or velocity and acceleration, and suggests it is possible for humans to respond to such composite variables, rather than directly to ordinary 'engineering variables'. This motivates the further analysis of Section V.

V. SOURCES OF FRACTIONALITY IN HUMAN-MACHINE SYSTEMS

Real-world plants should be uncomplicated to control, so levels of fractionality are likely to be low for most systems [51]. Nevertheless, the possible sources of fractionality in real-world man-machine systems are analyzed in this section by considering the various subsystems. In particular, as the motivation behind this research is its potential application to characterizing driver behavior, the case in which the plant is a ground vehicle is principally considered. Further, the possibility that human operators themselves introduce fractionality in the man-machine control loop is also studied.

A. PLANT DYNAMICS

To test the extent to which vehicle response can be considered fractional, the parameters of a fractional linear bicycle model were fitted with data obtained by running a simulation with CarMaker® [52], a high fidelity simulation tool used extensively in the industry. Details on the derivation of a fractional
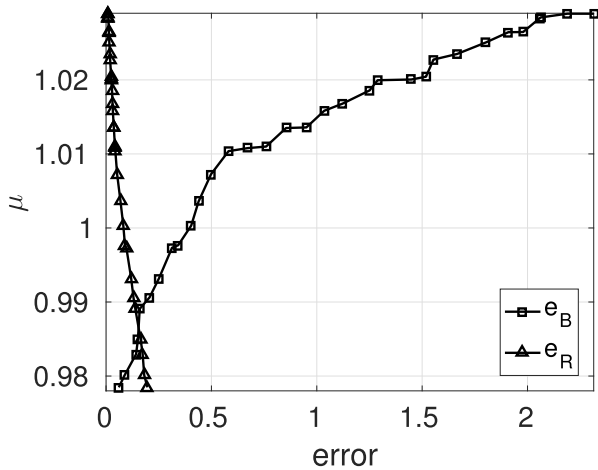
FIGURE 9. Relative errors e_B and e_R from (28a) and (28b) vs. the fractional parameter μ. Each point corresponds to a member of the Pareto frontier, which contains the potential optimal solution alternatives yielded by the optimization algorithm. The two curves intersect at $\mu \approx 0.987$ with $e_B = e_R \approx 0.154$.

FIGURE 10. Relationship between the order of the plant (12) and the fractional-order ν that brings maximal correlation between $_0D_t^{\nu}e(t)$ and $c(t)$ for the recorded events.

bicycle model, data recording and the optimization process can be found in the appendix.

A multi-objective optimization process was employed to fit the parameters of a linear bicycle model with additional fractional dynamics. The model consisted of two dynamical equations: one equation for the body slip angle and the other for the yaw rate of the vehicle. Two objective functions, e_B and e_R, represent the relative error between the simulated data and each of the equations. The fractionality was introduced in the model with an additional parameter μ. The optimized values of the Pareto frontier are displayed in Fig. 9. The fitted parameters show that the fractional bicycle model is very near to the non-fractional case ($\mu = 1$) with $\mu = 0.987$, although the fractional model fits better the transient phase in the step response (see appendix). According to this analysis, ground vehicles may introduce a certain degree of fractionality in the human-machine system, but not to the same degree as in the experiments of Section IV. This fractionality is likely to derive from the elasto-kinematics of the tyre, the steering system or the suspension systems, and may be more significant for heavy vehicles or for vehicles driven off-road.

B. HUMAN-OPERATOR DYNAMICS

Section II-C suggested two mechanisms involved in visual perception that can imply fractionality within the human operator: trans-saccadic memory and vestibulo-oculomotor neurons. Regarding the first, it has been reported that the duration of a saccade is generally less than 100 ms [53]. This gives an approximation of the memory integration time of this process.

There is another way in which the visual system may introduce fractionality: perceived visual inputs are processed in different parts of the brain via a complex network of feedforward and feedback connections [54]. The neural visual pathway displays a peak in activation before any motor output
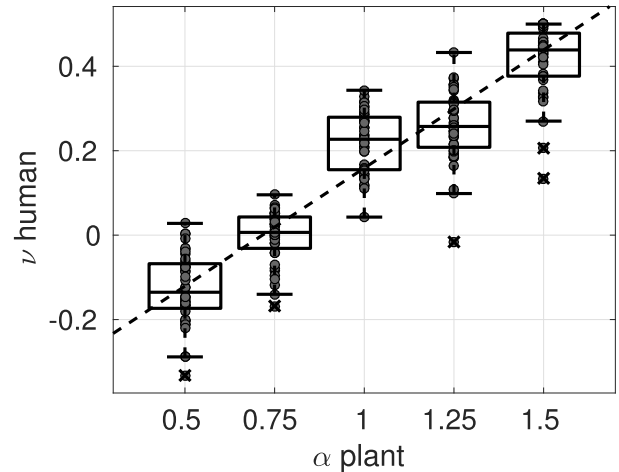
is performed [55]; neural processing of a perceived image until identification can take around 150 ms. Thus visual processing has a memory integration time comparable to that of the duration of a saccade.

Here the possibility that visual processing of the tracking error can be modeled with a fractional operator is considered For the 200 recorded events, a genetic algorithm was run that maximizes the correlation between $_0D_t^{\nu}e(t)$, the fractional derivative or integral of $e(t)$, and $c(t)$, the human operator manipulative control actions, by varying ν (Fig. 10). Through this method, it is inferred that the human operator response displays greater correlation to a delayed fractional error variable, rather than to an integer power of the differential operator; the time delay having been separately estimated by fitting the CO model to the data [26]. In the analysis, the median correlation was shown to increase from 0.758 to 0.816, when the fractional operator was added.

Further, the fractional error variable relates to the fractionality of the plant through an approximate linear relationship:

$$\nu = n\alpha + d_1 \equiv n\gamma + d_2 \qquad (24)$$

with $n = 0.56$, $d_1 = -0.40$ and $d_2 = 0.16$.

This result provides *indirect evidence for fractionality in the human controller*. Our interpretation is that the human operator responds to visually interpreted information with some level of fractionality, and that visual inputs for the tracking task can be modeled as a linear filter that takes into account sampled past observations (8) (Fig. 11).

C. DISCUSSION

Taking as benchmarks the CO model and the FCO model and the classical literature, it can be concluded that the overall human control response for non-fractional order plants is itself non-fractional. But human responses appear more highly correlated to fractionally integrated visual information. Further, in Section IV it was shown that humans are
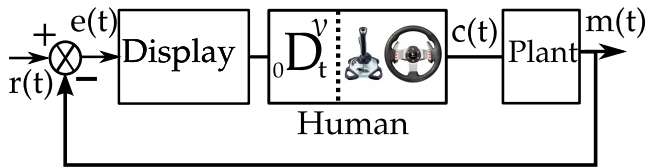
FIGURE 11. Suggested scheme by the analysis in the recorded data: The human-operator responds to an error variable that can be modeled with a fractional operator. The human operator compensates to produce a non-fractional response *c(t)* – when interacting with non-fractional plants – according the the FCO model.

able to reduce the fractionality of the whole human-machine system in about 70%. Considering that most real-world plants are non-fractional, this raises the question of why humans possess any skill to control and compensate fractional order plants. One explanation is that visual perception, muscular dynamics and the central nervous system contain memory aspects that can be described as a fractional process, and human neuromuscular responses can be characterized as a process that compensates this fractionality, yielding a non-fractional response. In order to interact with a non-fractional plant, the most convenient approach for the operator is to produce a non-fractional manipulative action. A mechanism of fractional compensation has previously been proposed for vestibulo-oculomotor neurons; in [3] it is contemplated that the fractional dynamics of motor neurons compensates the fractional dynamics of the eye. From the analysis presented here, a mechanism of fractional compensation is the most plausible explanation.

The mechanism of fractional compensation can occur in a number of different ways. One possibility is that it occurs in the muscular system. Fractional-order dynamics seem to be general in the muscular system [4] [56]. The musculoskeletal system is composed of viscoelastic polymers, which are known to be well modeled by fractional dynamics. In [25] the plausibility of driver steering control to be characterized by intermittent asymmetrical pulses was demonstrated. However, human steering output recordings appear to be smooth. The fractional aspects of the motor system can explain the transition between discrete pulses and smooth steering response. Regarding the fractional compensation, another possibility is that it occurs during the visual processing stage. However, without a complementary analysis of neural recordings the exact process of compensation cannot be fully characterized.

VI. CONCLUSIONS
The research presented in this paper is motivated towards the formulation of biofidelic human-control models, for example in the control of ground vehicles. This paper has examined the characteristics of human control, in the presence of fractional order dynamics. The investigation was conducted by analyzing the closed-loop control actions of humans (data-driven modeling) to track the response of various plants – of fractional and non-fractional order – subject to quasi-random disturbances.

It was first shown that the classical Crossover (CO) model does not perform satisfactorily when fractional-order plants are considered. A generalization of this model, the Fractional Crossover (FCO) model, was proposed and validated with human data. For the case when the plant is non-fractional, the FCO model coincides with the CO model. The FCO model *shows that humans can compensate for fractionality in the controlled plant.* Further, strongest correlations were observed between the human response and a fractional derivative of the input error; and the order of the optimal fractional operator, was seen to depend on the order of the plant through an approximately linear relationship.

These findings lead the authors to advance a series of plausible conjectures regarding human-control; it is proposed the hypothesis that visual cues in tracking tasks are composite motion variables, that can be represented by fractional derivatives of the standard engineering variables. In addition, the approximated but consistent linear relationships observed, are hypothetized to be the result of the adaptation by the human operator, *providing evidence of inherent fractionality within the human controller.* The resulting hypothesis is that humans integrate spatio-temporal visual information to determine the required response, and this effect can be represented with fractional variables.

The research has clearly shown that humans compensate for fractional order dynamics, at least partially. One possible interpretation is that visual perception and neuromuscular dynamics have the characteristics of a fractional-order process, and further visual processing or muscular response can reduce the associated fractionality. Perhaps this is the underlying basis for the fractional order compensation seen in the test results.

The results here presented have been tested on a particular type of plant, thus cannot be generalized to every human-control setting. But the fact that they coincide with the CO model for the non-fractional case suggests that the experimental approach is correct.

One difficulty in this proposition is the unfeasibility in determining the exact location of the fractionality in the system, simply by analyzing the motor response of the human. Thus several potential sources of fractionality were considered. As exemplified by the handling dynamics of a ground vehicle, real world plants have very low levels of fractionality.

In real-world control problems, the visual stimulus is more complex than a single moving dot. In this article, the biological or optical aspects of visual perception have been intentionally set aside, so that patterns in data are more conveniently identified. Future research is to be aimed towards the design of biofidelic human-control models which do include more realistic visual stimuli, in particular the road scene used for the steering control in ground vehicles. This will aid the development of effective shared-control systems and cyber-physical systems, for example in the vehicle industry. Moreover, such models may provide insights to guide neuroscience about the functional performance of the central nervous sys-
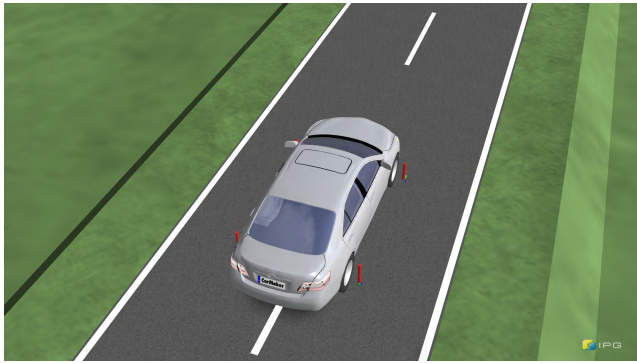
FIGURE 12. Ground vehicle simulation representing the characteristics of a Toyota Camry 2006 with a band limited random steering angle, in a straight road.

TABLE 3. Mathematical symbols, variables and parameters.

Symbol	Meaning
$\mathcal{L}\{\cdot\}$	Laplace transform
s	Complex frequency
$_0D_t^\xi f(t)$	Fractional derivative ($\xi > 0$) or integral ($\xi < 0$) of f of order $\xi \in \mathbb{R}$.
$\Gamma(\cdot)$	Gamma function
h	Differintegration step
$\mathbb{N}, \mathbb{Z}, \mathbb{R}, \mathbb{C}$	Natural, Integer, Real and Complex numbers respectively
ω_c	Crossover frequency
τ	Effective time delay
T	Time constant of the plant
α	Fractional order plant
γ	Plant fractionality
ν	Fractional order (human)
λ	Fractional order human + plant
Y_h^λ	Human transfer function
Y_p^α	Plant transfer function
$r(t)$	Forcing function
$e(t)$	Control loop error
$h(t)$	Human response
$m(t)$	Plant response
β	Body slip angle
r	Yaw rate
δ_f	Steering angle
M	Vehicle mass
U	Vehicle speed
I	Vehicle yaw moment of inertia
$C_{\alpha f}$	Vehicle front cornering stiffness
$C_{\alpha r}$	Vehicle rear cornering stiffness
l_f	Distance from vehicle center of gravity to front axle
l_r	Distance from vehicle center of gravity to rear axle
e_B, e_R	Optimization error for body slip angle and yaw rate respectively

tem, and so complement research at the neural level, e.g using fMRI or EEG data.

APPENDIX
FRACTIONAL MODELING OF A VEHICLE

To estimate the level of fractionality in a complex road vehicle, as modeled by a simple fractional order system, data was obtained by running a simulation in CarMaker® in Fig. 12. The simulation represented a Toyota Camry 2006 vehicle
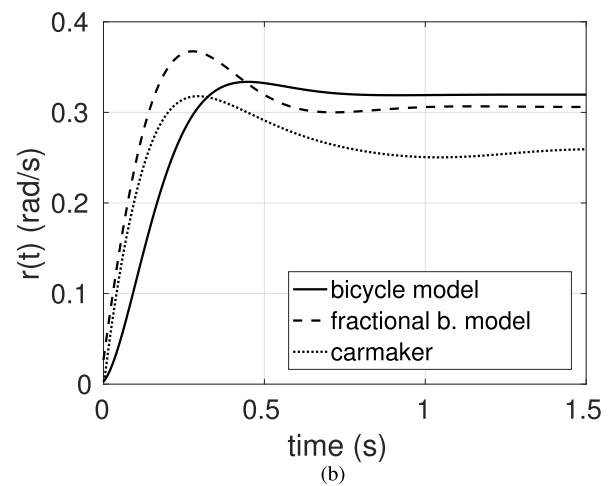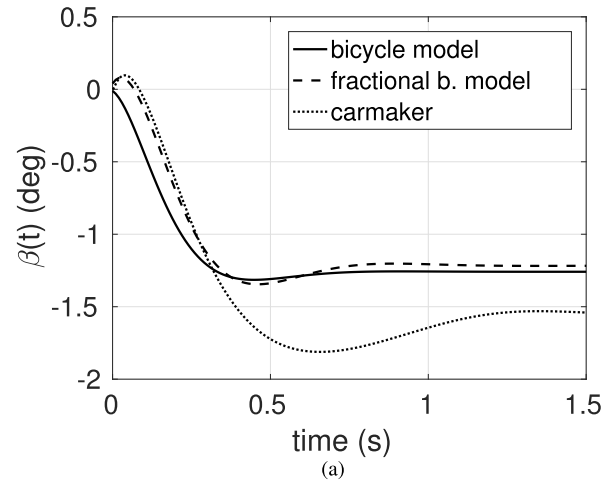
FIGURE 13. Step response for the optimized solution for (27) with $\mu = 1$ (non-fractional), $\mu = 0.987$ and for the CarMaker® simulation setup: (a) body slip angle and (b) yaw rate. While the transient is slightly different for $\mu \neq 1$ – more overshoot is present in fractional case – the steady state response is very similar for both models. The step input is of $\delta_f = 0.05$ rad.

with a band limited random steering angle, in a straight road of non-limiting width. The recorded signals were the body slip angle $\beta(t)$ and the yaw rate $r(t)$. The data were sampled at 50 Hz and the signal had a duration of 100 min.

The parameters of a linear bicycle model – and of a fractional version of this model – were fitted with the data. The considered bicycle model (from [57]) is:

$$\begin{bmatrix} \dot{\beta} \\ \dot{r} \end{bmatrix} = -\begin{bmatrix} L_0/MU & 1 + L_1/MU^2 \\ L_1/I & L_2/IU \end{bmatrix}\begin{bmatrix} \beta \\ r \end{bmatrix} + \begin{bmatrix} C_{\alpha f}/MU \\ l_f C_{\alpha f}/I \end{bmatrix}\delta_f \quad (25)$$

with

$$\begin{cases} L_0 = C_{\alpha f} + C_{\alpha r} \\ L_1 = l_f C_{\alpha f} + l_r C_{\alpha r} \\ L_2 = l_f^2 C_{\alpha f} + l_r^2 C_{\alpha r} \end{cases} \quad (26)$$

and where $C_{\alpha f}$ and $C_{\alpha r}$ are the *axle cornering stiffness* for the front and rear axle respectively, M is the mass of the

vehicle, U the speed – which was chosen to be constant at $100 \, km/h$, l_f and l_r are the distances from the center of gravity of the vehicle to the front and rear axle respectively, I the yaw moment of inertia and δ_f the front steering angle. A fractional version of the model can be rewritten as a transfer function with an additional parameter μ:

$$
\begin{bmatrix} B \\ R \end{bmatrix} = \begin{bmatrix} \frac{C_{\alpha f}(IUs^{\mu} - Ml_f U^2 + L_2 - L_1 l_f)}{IMU^2 s^{2\mu} + (IL_0 U + L_2 MU)s^{\mu} + L_0 L_2 - L_1^2 - L_1 MU^2} \\ \frac{C_{\alpha f} U(MUl_f s^{\mu} + L_0 l_f - L_1)}{IMU^2 s^{2\mu} + (IL_0 U + L_2 MU)s^{\mu} + L_0 L_2 - L_1^2 - L_1 MU^2} \end{bmatrix} \Delta_f
$$
(27)

where $\mathcal{L}\{\beta(t)\} = B(s)$, $\mathcal{L}\{r(t)\} = R(s)$ and $\mathcal{L}\{\delta_f(t)\} = \Delta_f(s)$. For $\mu = 1$ (27) is identical to (25).

A multi-objective optimization process through a genetic algorithm is used with a grey-box modeling approach: It is pre-assumed some knowledge about the data – it follows approximately (27) with known M, U, l_f, l_r and I – but as $C_{\alpha f}$ and $C_{\alpha r}$ are more difficult to approximate experimentally and μ is unknown, the genetic algorithm will fit L_0, L_1, L_2, $C_{\alpha f}$ and μ. The bidimensional objective function for the optimization process is:

$$
e_B = \sqrt{\frac{1}{N} \sum_{\omega=0.1}^{2 \, \text{Hz}} \left| \frac{\hat{B}(j\omega) - B(j\omega)}{B(j\omega)} \right|^2}
$$
(28a)

$$
e_R = \sqrt{\frac{1}{N} \sum_{\omega=0.1}^{2 \, \text{Hz}} \left| \frac{\hat{R}(j\omega) - R(j\omega)}{R(j\omega)} \right|^2}
$$
(28b)

where $\hat{B}$ and $\hat{R}$ are the estimates of the frequency response of (27) and N the number of samples in the range 0.1-2 Hz. Thus the objective function is dimensionless. The step responses for each system are very similar, although the fractional model offers a better fit during the transient phase (Fig. 13). Both models present a less precise fit of the steady state response, possibly due to effects introduced by the steering compliance, which the bicycle model does not replicate.

REFERENCES

[1] G. Schirner, D. Erdogmus, K. Chowdhury, and T. Padir, "The future of human-in-the-loop cyber-physical systems," *Computer*, vol. 46, no. 1, pp. 36–45, Jan. 2013.

[2] T. J. Gordon and M. Lidberg, "Automated driving and autonomous functions on road vehicles," *Vehicle Syst. Dyn.*, vol. 53, no. 7, pp. 958–994, 2015.

[3] T. J. Anastasio, "The fractional-order dynamics of brainstem vestibulo-oculomotor neurons," *Biol. Cybern.*, vol. 72, no. 1, pp. 69–79, 1994.

[4] I. Tejado, D. Valério, P. Pires, and J. Martins, "Fractional order human arm dynamics with variability analyses," *Mechatronics*, vol. 23, no. 7, pp. 805–812, 2013.

[5] K. Kristinsson and G. A. Dumont, "System identification and control using genetic algorithms," *IEEE Trans. Syst., Man, Cybern.*, vol. 22, no. 5, pp. 1033–1046, Sep. 1992.

[6] Z. Huo, Y. Zhang, P. Francq, L. Shu, and J. Huang, "Incipient fault diagnosis of roller bearing using optimized wavelet transform based multi-speed vibration signatures," *IEEE Access*, vol. 5, pp. 19442–19456, 2017.

[7] R. J. Jagacinski and J. M. Flach, *Control Theory for Humans: Quantitative Approaches to Modeling Performance*. Boca Raton, FL, USA: CRC Press, 2003.

[8] O. Lappi, "Future path and tangent point models in the visual control of locomotion in curve driving," *J. Vis.*, vol. 14, no. 12, p. 21, 2014.

[9] A. J. Grunwald and S. J. Merhav, "Vehicular control by visual field cues-analytical model and experimental validation," *IEEE Trans. Syst., Man, Cybern.*, vol. SMC-6, no. 12, pp. 835–845, Dec. 1976.

[10] D. T. McRuer, D. H. Weir, H. R. Jex, R. E. Magdaleno, and R. W. Allen, "Measurement of driver-vehicle multiloop response properties with a single disturbance input," *IEEE Trans. Syst., Man, Cybern.*, vol. SMC-5, no. 5, pp. 490–497, Sep. 1975.

[11] S. Baron and D. L. Kleinman, "The human as an optimal controller and information processor," *IEEE Trans. Man-Mach. Syst.*, vol. MMS-10, no. 1, pp. 9–17, Mar. 1969.

[12] V. Mnih et al., "Human-level control through deep reinforcement learning," *Nature*, vol. 518, no. 7540, pp. 529–533, 2015.

[13] C. C. MaCadam, "Understanding and modeling the human driver," *Vehicle Syst. Dyn.*, vol. 40, nos. 1–3, pp. 101–134, 2003.

[14] M. Plöchl and J. Edelmann, "Driver models in automobile dynamics application," *Vehicle Syst. Dyn.*, vol. 45, nos. 7–8, pp. 699–741, 2007.

[15] C. C. MacAdam, "Application of an optimal preview control for simulation of closed-loop automobile driving," *IEEE Trans. Syst., Man, Cybern.*, vol. 11, no. 6, pp. 393–399, Jun. 1981.

[16] M. Kondo and A. Ajimine, "Driver's sight point and dynamics of the driver-vehicle-system related to it," SAE Tech. Paper 680104, 1968.

[17] G. Prokop, "Modeling human vehicle driving by model predictive online optimization," *Vehicle Syst. Dyn.*, vol. 35, no. 1, pp. 19–53, 2001.

[18] J. Rix and D. Cole, "Models of human learning applicable to the vehicle steering task," in *Proc. 6th Int. Symp. Adv. Vehicle Control*, 2002, pp. 1–6.

[19] D. D. Salvucci and R. Gray, "A two-point visual control model of steering," *Perception*, vol. 33, no. 10, pp. 1233–1248, 2004.

[20] D. T. McRuer, R. W. Allen, D. H. Weir, and R. H. Klein, "New results in driver steering control models," *Human Factors*, vol. 19, no. 4, pp. 381–397, 1977.

[21] C. C. MacAdam and G. E. Johnson, "Application of elementary neural networks and preview sensors for representing driver steering control behaviour," *Vehicle Syst. Dyn.*, vol. 25, no. 1, pp. 3–30, 1996.

[22] B. Huval et al. (2015). "An empirical evaluation of deep learning on highway driving." [Online]. Available: https://arxiv.org/abs/1504.01716

[23] A. Hollingworth, C. C. Williams, and J. M. Henderson, "To see and remember: Visually specific information is retained in memory from previously attended objects in natural scenes," *Psychonomic Bull. Rev.*, vol. 8, no. 4, pp. 761–768, 2001.

[24] S. Ostojic and N. Brunel, "From spiking neuron models to linear-nonlinear models," *PLoS Comput. Biol.*, vol. 7, no. 1, p. e1001056, 2011.

[25] M. Martínez-García, Y. Zhang, and T. Gordon, "Modeling lane keeping by a hybrid open-closed-loop pulse control scheme," *IEEE Trans. Ind. Informat.*, vol. 12, no. 6, pp. 2256–2265, Dec. 2016.

[26] M. Martínez-García and T. Gordon, "Human control of systems with fractional order dynamics," in *Proc. IEEE Int. Conf. Syst., Man, Cybern. (SMC)*, Oct. 2016, pp. 002866–002871.

[27] Y.-F. Pu and X. Yuan, "Fracmemristor: Fractional-order memristor," *IEEE Access*, vol. 4, pp. 1872–1888, 2016.

[28] Y.-F. Pu, "Measurement units and physical dimensions of fractance-part I: Position of purely ideal fractor in Chua's axiomatic circuit element system and fractional-order reactance of fractor in its natural implementation," *IEEE Access*, vol. 4, pp. 3379–3397, 2016.

[29] P. Szendro, G. Vincze, and A. Szasz, "Bio-response to white noise excitation," *Electro- Magnetobiol.*, vol. 20, no. 2, pp. 215–229, 2001.

[30] K. Clayton and B. B. Frey, "Studies of mental 'noise'," *Nonlinear Dyn., Psychol., Life Sci.*, vol. 1, no. 3, pp. 173–180, 1997.

[31] K. S. Miller and B. Ross, *An Introduction to the Fractional Calculus and Fractional Differential Equations*. Hoboken, NJ, USA: Wiley, 1993.

[32] K. Diethelm, *The Analysis of Fractional Differential Equations: An Application-Oriented Exposition Using Differential Operators of Caputo Type*. Heidelberg, Germany: Springer, 2010.

[33] I. Podlubny, *Fractional Differential Equations: An Introduction to Fractional Derivatives, Fractional Differential Equations, to Methods of Their Solution and Some of Their Applications*, vol. 198. San Diego, CA, USA: Academic, 1998.

[34] S. Bitzer, H. Park, F. Blankenburg, and S. J. Kiebel, "Perceptual decision making: Drift-diffusion model is equivalent to a Bayesian model," *Frontiers Hum. Neurosci.*, vol. 8, p. 102, Feb. 2014.

[35] C. Lubich, "Discretized fractional calculus," *SIAM J. Math. Anal.*, vol. 17, no. 3, pp. 704–719, 1986.

[36] S.-Y. Shao, M. Chen, and Q.-X. Wu, "Stabilization control of continuous-time fractional positive systems based on disturbance observer," *IEEE Access*, vol. 4, pp. 3054–3064, 2016.

[37] F. Hassan and A. Zolotas, "Impact of fractional order methods on optimized tilt control for rail vehicles," *Fract. Calculus Appl. Anal.*, vol. 20, no. 3, pp. 765–789, 2017.

[38] D. T. McRuer and H. R. Jex, "A review of quasi-linear pilot models," *IEEE Trans. Hum. Factors Electron.*, vol. HFE-8, no. 3, pp. 231–249, Sep. 1967.

[39] D. T. McRuer and E. S. Krendel, "Mathematical models of human pilot behavior," DTIC Document, Neuilly-sur-Seine, France, Tech. Rep. AGARD-AG-188, 1974.

[40] D. T. McRuer, "Human dynamics in man-machine systems," *Automatica*, vol. 16, no. 3, pp. 237–253, May 1980.

[41] T. J. Gordon, "Nonlinear crossover model of vehicle directional control," in *Proc. Amer. Control Conf. (ACC)*, 2009, pp. 451–456.

[42] C. W. Clifford and M. R. Ibbotson, "Fundamental mechanisms of visual motion detection: models, cells and functions," *Prog. Neurobiol.*, vol. 68, no. 6, pp. 409–437, 2002.

[43] A. Hollingworth, A. M. Richard, and S. J. Luck, "Understanding the function of visual short-term memory: Transsaccadic memory, object correspondence, and gaze correction," *J. Experim. Psychol., General*, vol. 137, no. 1, p. 163, 2008.

[44] E. Matin, "Saccadic suppression: A review and an analysis," *Psychol. Bull.*, vol. 81, no. 12, pp. 899–917, 1974.

[45] L. Debnath, "Recent applications of fractional calculus to science and engineering," *Int. J. Math. Math. Sci.*, vol. 54, no. 54, pp. 3413–3442, 2003.

[46] J. W. Senders and M. Cruzen, "Tracking performance on combined compensatory and pursuit tasks," Wright Air Develop. Center, Air Res. Develop. Command, United States Air Force, Washington, DC, USA, Tech. Rep. 52-39, 1952.

[47] R. W. Pew, J. C. Duffendack, and L. K. Fensch, "Sine-wave tracking revisited," *IEEE Trans. Hum. Factors Electron.*, vol. HFE-8, no. 2, pp. 130–134, Jun. 1967.

[48] R. W. Pew, "Some history of human performance modeling," in *Integrated Models of Cognitive Systems*. Oxford, U.K.: Oxford Univ. Press, 2007, pp. 29–44.

[49] B. Andonian, W. Rauch, and V. Bhise, "Driver steering performance using joystick vs. steering wheel controls," *SAE Trans.*, vol. 112, no. 6, pp. 1–12, 2003.

[50] R. W. Allen, H. R. Jex, D. T. McRuer, and R. J. DiMarco, "Alcohol effects on driving behavior and performance in a car simulator," *IEEE Trans. Syst., Man, Cybern.*, vol. SMC-5, no. 5, pp. 498–505, Sep. 1975.

[51] Y. Chen, I. Petráš, and D. Xue, "Fractional order control—A tutorial," in *Proc. Amer. Control Conf. (ACC)*, 2009, pp. 1397–1411.

[52] *CarMaker Version 5.0.1*. Accessed: Jul. 20, 2015. [Online]. Available: http://ipg.de/

[53] A. T. Bahill, M. R. Clark, and L. Stark, "The main sequence, a tool for studying human eye movements," *Math. Biosci.*, vol. 24, nos. 3–4, pp. 191–204, 1975.

[54] J. Bullier, "Integrated model of visual processing," *Brain Res. Rev.*, vol. 36, nos. 2–3, pp. 96–107, 2001.

[55] S. Thorpe, D. Fize, and C. Marlot, "Speed of processing in the human visual system," *Nature*, vol. 381, no. 6582, p. 520, 1996.

[56] R. L. Magin, "Fractional calculus models of complex dynamics in biological tissues," *Comput. Math. Appl.*, vol. 59, no. 5, pp. 1586–1593, 2010.

[57] M. Abe, *Vehicle Handling Dynamics: Theory and Application*. Oxford, U.K.: Butterworth-Heinemann, 2015.

MIGUEL MARTÍNEZ-GARCÍA received the B.Sc. degree in mathematics and the M.Sc. degree in advanced mathematics and mathematical engineering from the Polytechnic University of Catalonia, Barcelona, Spain, in 2013 and 2014, respectively. He is currently pursuing the Ph.D. degree in biofidelic driver behavior modeling with the University of Lincoln, U.K. His research interests include human control, man–machine systems, machine learning, artificial intelligence, human performance modeling and applied mathematics in general.

TIMOTHY GORDON received the B.A. and M.A. degrees in mathematics from the University of Cambridge, U.K., in 1974 and 1975, respectively, and the Ph.D. degree in applied mathematics from the Department of Applied Mathematics and Theoretical Physics, University of Cambridge, in 1983. He has held several senior academic posts, including a Professor of mechanical engineering with the University of Michigan, Ann Arbor, USA, and a Ford Professor of automotive engineering with the University of Loughborough, U.K. He is currently the Head of the School of Engineering, University of Lincoln, U.K. He is a Visiting Professor with Tongji University, China. He is the Vice President of the International Association for Vehicle System Dynamics and the Co-Chair of the IEEE Technical Committee on Vehicle Intelligent Control Systems.

LEI SHU (SM'16) is currently a Lincoln Professor with the University of Lincoln, U.K. and a Distinguished Professor with Nanjing Agricultural University, China. He is the Director of the NAU-Lincoln Joint Research Center of Intelligent Engineering. He has authored over 350 papers in related conferences, journals, and books in the area of sensor networks. His main research field is wireless sensor networks. He has served as a TPC Member for over 150 conferences, such as ICDCS, DCOSS, MASS, ICC, GlobeCom, ICCCN, WCNC, and ISCC. He received the GlobeCom 2010 and the ICC 2013 Best Paper Award and the IEEE Systems Journal 2017 Best Paper Award. He has served as the Co-Chair for more than 50 international conferences and workshops, such as IWCMC, ICC, ISCC, ICNC, and Chinacom. He has served as the Symposium Co-Chair for IWCMC 2012 and ICC 2012, the General Co-Chair for Chinacom 2014, Qshine 2015, CollaborateCom 2017, and Mobiquitous 2018, and a Steering and the TPC Chair for InisCom 2015.

● ● ●